# Atomic structure of Yb/Si(100)(2×6): Interrelation between the silicon dimer arrangement and Si 2*p* photoemission line shape

M. Kuzmin,[1,2,*] M. P. J. Punkkinen,[1,3] P. Laukkanen,[1,4] R. E. Perälä,[1] V. Tuominen,[1] J. J. K. Lång,[1] M. Ahola-Tuomi,[1] J. Dahl,[1] T. Balasubramanian,[5] B. Johansson,[3,6] L. Vitos,[3,6,7] and I. J. Väyrynen[1]

[1]*Department of Physics, University of Turku, FIN-20014 Turku, Finland*

[2]*Ioffe Physical-Technical Institute, Russian Academy of Sciences, St. Petersburg 194021, Russian Federation*

[3]*Applied Materials Physics, Department of Materials Science and Engineering, Royal Institute of Technology, SE-10044 Stockholm, Sweden*

[4]*Optoelectronics Research Centre, Tampere University of Technology, FIN-33101 Tampere, Finland*

[5]*MAX-lab, Lund University, SE-221 00 Lund, Sweden*

[6]*Condensed Matter Theory Group, Physics Department, Uppsala University, SE-75121 Uppsala, Sweden*

[7]*Research Institute for Solid State Physics and Optics, P.O. Box 49, H-1525 Budapest, Hungary*

(Received 28 May 2010; published 3 September 2010)

Combining photoelectron spectroscopy and density-functional theory calculations, we have studied the atomic geometry of Yb/Si(100)(2×6) reconstruction and the mechanisms responsible for its stabilization as well as the influence of this reconstruction on Si 2*p* core-level photoemission. The analysis of measured and calculated surface core-level shifts supports the recently proposed model of the Yb/Si(100)(2×6). It involves, in agreement with valence-band measurements, unbuckled (symmetrical) silicon dimers, leading to unusually narrowed Si 2*p* line shape as compared to those of related systems. The origin of the symmetrical dimers in the (2×6) structure is discussed in the context of previous results in literature.

DOI: 10.1103/PhysRevB.82.113302 PACS number(s): 68.43.Fg, 68.35.B−, 68.43.Bc, 79.60.−i

Silicon surfaces reconstruct in many different ways, and knowledge of their atomic structure plays a key role in understanding and controlling various phenomena, such as the adsorption, self-assembly, and epitaxial growth. One of the most powerful techniques to examine the surface atomic structure is core-level photoelectron spectroscopy combined with *ab initio* surface core-level shift (SCLS) calculations. In general, such shifts arise from the redistribution of valence-electron density at surface atoms and reflect changes in bonding configuration and charge state of these atoms as compared to the bulk atoms. In particular Si 2*p* core-level is very sensitive to the dimer buckling on clean Si(100)$p(2\times1)$ and $c(4\times2)$ surfaces, where the core-level binding-energy difference of dimer-down and dimer-up atoms is more than 0.5 eV and the SCLS component related to the up atom is shifted about 0.5 eV toward the lower binding energy relative to the bulk emission.[1–5] Clearly, the dimer buckling has a significant impact on the broadening of Si 2*p* photoemission line shape.

Recently, the atomic structure of Si(100) with submonolayer rare earth (RE) and Ba adsorbates has been thoroughly studied by density-functional theory (DFT) calculation.[6] It has been shown that fully relaxed atomic structures of Yb and Eu/Si(100)(2×3) [the coverage is 1/3 monolayer (ML) (Ref. 7)] involve both buckled (asymmetric) and unbuckled (symmetrical) silicon dimers, which is believed to result in relatively broad Si 2*p* photoemission in Refs. 8 and 9. In contrast, an energetically favorable structure of Yb/Si(100)(2×6) at 1/2 ML is not found to contain buckled dimers.[6] As shown in Fig. 1, it features unbuckled, mutually orthogonal, dimers formed by the first-layer Si atoms *b*1 and topmost-layer Si atoms *a*. Such a structure gives rise to a good agreement between the measured[10,11] and calculated scanning tunneling microscopy (STM) images (Ref. 6). However, no spectroscopic support has been so far reported for this model. Meanwhile, one can expect that the Si 2*p* binding-energy splitting of the dimer-up and dimer-down atoms is eliminated after the dimer symmetrization, leading to the narrowed Si 2*p* emission from Yb/Si(100)(2×6), which itself can be an interesting issue shedding light on ties of the surface structure and the Si 2*p* line shape. Moreover, the Yb/Si(100)(2×6) reconstruction can be considered as a precursor state for the ytterbium disilicide ($YbSi_{2-x}$),[11] which is a very promising material for the Schottky barrier source/drain contacts of N-channel metal-oxide-semiconductor field-effect transistors (Ref. 12). Thus, the atomic-scale insight into the structural arrangement of Yb/Si(100)(2×6) is also practically important.

In this Brief Report, we present experimental and DFT Si 2*p* data, together with Yb 4*f* and valence-band (VB) photoemission, for the Yb/Si(100)(2×6), which give support to the model of Fig. 1. These findings allows us to identify this surface as a particular case of RE/Si(100) reconstruction that demonstrates relatively small SCLS due to a specific Si arrangement.

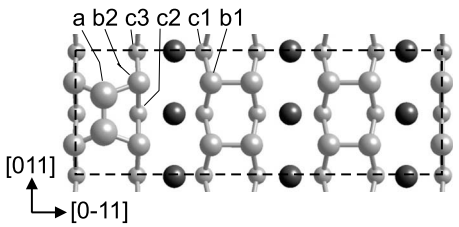


FIG. 1. The atomic model of Yb/Si(100)(2×6). The unit cell is outlined. The Yb atoms are shown by large black balls. The notations "*a*," "*b*," and "*c*" denote the Si atoms in the topmost, first, and second layers.

 

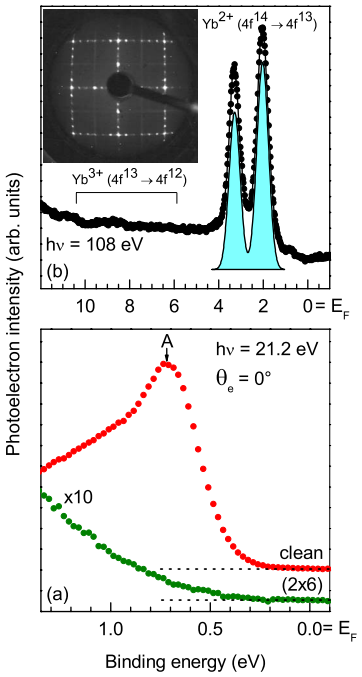


FIG. 2. (Color online) (a) Normal-emission valence spectra measured from the clean Si and $(2\times6)$ reconstruction with the photon energy $h\nu$=21.2 eV at 300 K. The spectra are normalized to the background intensity. The intensity of the $(2\times6)$ spectrum is multiplied by a factor of 10. (b) Yb $4f$ spectrum from the Yb/Si(100)$(2\times6)$ measured with $h\nu$=108 eV at 100 K. The raw data are represented by solid circles. The Yb $4f^{13}$ final state is fitted by a single component shown by shadowed spin-orbit-split doublet. The inset illustrates the $(2\times6)$ LEED pattern at 100 K. The electron energy is 45 eV.

The measurements were performed at the MAX-lab synchrotron radiation facility (beamline I4 at MAX-III) in Lund, Sweden. The Si $2p$ and Yb $4f$ spectra were acquired at 100 K by the SPECS Phoibos 100 analyzer with an acceptance angle of $\pm8°$ and the overall energy resolution of about 75 meV. The VB spectra were taken at 300 K using the ARUPS-10 analyzer with the angular and energy resolution of $\pm2°$ and 80 eV, respectively. The Si samples were cut from P-doped (100) wafer ($n$-type, 1–2 Ω cm) and cleaned *in situ* by the standard procedure (Ref. 11). After the cleaning sharp $(2\times1)$ and $c(4\times2)$ low-energy electron-diffraction (LEED) patterns were observed at 300 K and 100 K, respectively. Ytterbium was evaporated onto Si at 300 K, followed by annealing at 800 K.

Figure 2(a) illustrates changes in the VB region of the Si surface upon the formation of the Yb-induced $(2\times6)$ reconstruction. The dominant feature of the clean substrate [the top spectrum in Fig. 2(a)] is a sharp peak (labeled A) at about 0.7 eV, which is due to the dangling bond surface state associated with the up atom of the asymmetric dimers (see, e.g., Ref. 13). When the $(2\times6)$ reconstruction is formed, this state is clearly suppressed [the bottom spectrum in Fig. 2(a)], indicating that the asymmetric dimer arrangement is broken.

Yb $4f$ spectrum and LEED pattern from the Yb/Si(100)$(2\times6)$ at 100 K are shown in Fig. 2(b). In agreement with Ref. 6, the Yb atoms are completely divalent, and the Yb $4f^{13}$ final state doublet is fitted by a single component with a spin-orbit splitting (SOS) of 1.2 eV, suggesting similar bonding sites for the Yb atoms. The $\times2$ periodicity appears in the form of half-order LEED streaks that have a similar intensity at 300 and 100 K. The lack of $\frac{1}{2}$-order spots is consistent with earlier observations,[11] and it can be explained in terms of the "out-of-the-phase" shift of topmost-layer Si dimer rows in Fig. 1.

Figure 3 shows normalized Si $2p$ spectra (filled dots) and their decompositions (solid lines) for the clean Si(100)$c(4\times2)$ surface (left panel) and the $(2\times6)$ reconstruction (right panel) at 100 K and various $h\nu$ and emission angles ($\theta_e$). As the Si $2p$ fitting procedure for the Si(100)$c(4\times2)$ is well known,[3–5] the analysis of the clean spectrum in Fig. 3 provides justified parameters for fitting the $(2\times6)$ spectra. For the clean substrate, we found seven spin-orbit split Voigt components ($B$, $S_u$, $C$, $S_d$, $S'$, $D$, and $L$) (shadowed doublets). The SCLS of $S_u$, $C$, $S_d$, $S'$, $D$, and $L$ are −0.48, −0.18, 0.06, 0.24, 0.39, and 1.35 eV relative to $B$. The Lorentzian full width at half maximum (LW), which varies in different studies (Ref. 4), is determined from the analysis of the lower-binding-energy tail of $S_u$ that has no overlap with the other components. The value was found to be 67 meV and then fixed for all the components. The SOS is 610 meV. The branching ratio (BR) is allowed to vary around 0.50 within 10% due to the possible diffraction effects. The Gaussian widths (GWs) of $B$, $S_u(S_d)$, $C$, $S'$, $D$, and $L$ are 175 meV, 203 meV, 188 meV, 192 meV, 202 meV, and 346 meV, respectively. The above results are consistent with Refs. 3–5 and the origin of identified components was interpreted *ibidem*. We note that very grazing emission angle (80°) allowed us to highly enhance the surface sensitivity and obtain Si $2p$ emis-

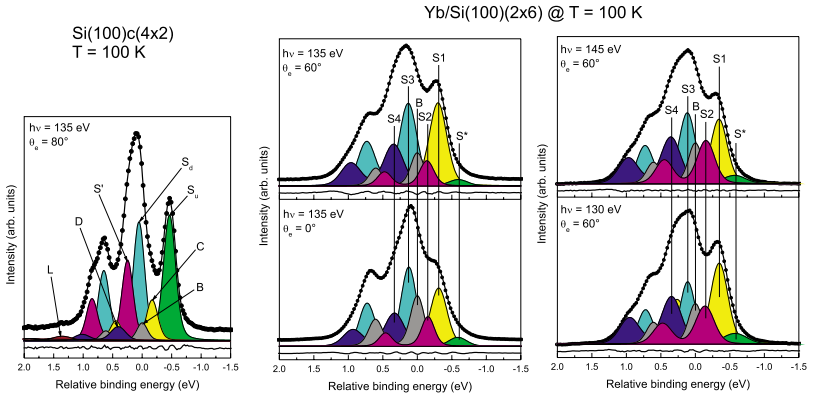


FIG. 3. (Color online) Si $2p$ spectra of clean Si(100)$c(4\times2)$ ($h\nu$=135 eV and $\theta_e$=80°) and Yb/Si(100)$(2\times6)$ ($h\nu$=130, 135, and 145 eV; $\theta_e$=0° and 60°). The spectra are taken at 100 K. The fitting results (SCLS components) are shown by shadowed doublets. The $(2\times6)$ spectra are normalized by their maxima.

sion which is largely contributed by the topmost layer [i.e., the up ($S_u$) and down ($S_d$) atoms of the asymmetric dimers]. The bulk contribution ($B$) is so low that the spectrum is almost completely due to the first three atomic layers and has almost pure surface origin.

To fit the $(2\times6)$ spectra, at least five spin-orbit-split components ($B$, $S1$, $S2$, $S3$, and $S4$) are required. They can reasonably reproduce these spectra except for their lower-binding-energy tail. Such a fitting scheme cannot be improved even by an increase in GW. Therefore, a minor (sixth) component $S^*$ was added. The results are shown in the right panel of Fig. 3. The five SCLS are −0.32($S1$), −0.15($S2$), 0.12($S3$), 0.34($S4$), and −0.58 eV ($S^*$). The GW of $B$ is 179 meV, and that of the surface components varies between 209 and 277 meV. The LW, SOS, and BR are the same as for the clean surface. It is essential that the SCLS and GW of $S1$, $S2$, $S3$, and $S4$ are very similar in the two fitting schemes with five and six components, and therefore, we conclude that the $S1$, $S2$, $S3$, and $S4$ are due to the $(2\times6)$ reconstruction irrespective of the fitting scheme. In contrast, the origin of $S^*$ is clearly different because its intensity is significantly smaller than those of $S1-S4$ and it is moreover not reproduced by DFT calculations, as seen below. The $S^*$ most likely originates from defects on the Yb/Si(100) surface, as found by STM (Ref. 11). The further introducing of additional components does not improve the fitting.

To interpret the $S1-S4$, theoretical SCLS were calculated. The calculations were performed by using Vienna *ab initio* simulation package (VASP),[14] applying the projector augmented wave method[15] and the local-density approximation of Ceperley and Alder,[16] as parametrized by Perdew and Zunger,[17] for the atomic structure of Yb/Si(100)$(2\times6)$ which was fully optimized by utilizing conjugate-gradient minimization of the total energy with respect to the atomic coordinates in Ref. 6. The SCLS were evaluated by using the average electrostatic potential at the core of the Si atoms.[18] The bulk reference value was obtained by averaging from the layers 5–7. The comparison of calculated and experimental data is given in Fig. 4(a). The vertical bars point out the values of SCLS. In the bottom panel the bar height is proportional to the intensity of measured SCLS at $h\nu=135$ eV and $\theta_e=0°$. In the middle and top panels the bar height is proportional to the number of corresponding Si atoms in the $(2\times6)$ unit cell in Fig. 1. Within the initial state model, the calculated SCLS are 0.06 eV for the top-layer Si atom $a$, 0.25 and −0.18 eV for the first-layer Si atoms $b1$ and $b2$, and −0.07, 0.25, and 0.28 eV for the second-layer Si atoms $c1$, $c2$, and $c3$, respectively. The energy ranges of these SCLS and measured ones agree very well (−0.25 eV to +0.28 eV and −0.32 eV to 0.34 eV, respectively). Taking into account the complete screening effects in the final state model, the SCLS are −0.50 eV for the atom $a$, −0.37 eV both for $b1$ and $b2$, and −0.13, +0.16, and +0.18 eV for $c1$, $c2$, and $c3$, respectively. [Note that there is an uncertainty (~0.1 eV) in evaluating the final state SCLS due to the nonaccurate bulk reference value.[19]] Roughly, the final state values tend to move systematically toward the lower binding energy as compared to the respective initial state values while the general trend (i.e., the energy difference between the highest and lowest SCLS) remains the same. A more

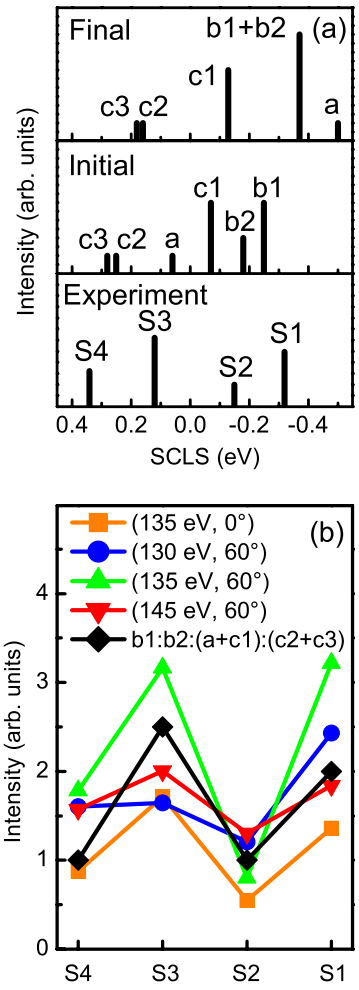


FIG. 4. (Color online) Comparison of (a) calculated and experimental SCLS values and (b) the intensity ratio of $S1:S2:S3:S4$ at various experimental conditions ($h\nu, \theta_e$) and the number ratio of respective Si atoms. For details see the text.

detailed analysis, however, shows that the final state model describes the $(2\times6)$ spectra poorer than the initial state model, and also that the effect of shifting final state values toward the lower binding energy is overestimated. Hence, we further consider the initial state scenario for the $(2\times6)$ surface. This differs from the case of clean Si(100) where the Si $2p$ data are better interpreted within the final state scheme (Refs. 2 and 5). It is believed that the initial state model is reasonable for the Yb/Si(100)$(2\times6)$ because of charge redistribution at this reconstruction (see below), leading to the symmetrical dimer arrangement. We notice that the screening effects are most significant for the topmost-layer atoms $a$ in Fig. 1. This agrees with the final state results for the clean Si(100) where the gain in relaxation energy is largest for the topmost atoms, especially for the down atom of the asymmetric dimer.[2,5]

It is also seen that the intensity ratios of measured SCLS correlate with the number ratio of the Si atoms that are suggested to be the origins of these SCLS in Fig. 4(a). Based on the initial state results, we assume that the Si atoms $b1$ contribute to $S1$, the Si atoms $b2$ to $S2$, the Si atoms $a$ and $c1$ to $S3$, and the Si atoms $c2$ and $c3$ to $S4$. Then the number ratio

of $b1:b2:(a+c1):(c2+c3)$ (4:2:5:2) is well consistent with the intensity ratios of $S1$, $S2$, $S3$, and $S4$ at different experimental conditions, as shown in Fig. 4(b). For example, the $S1:S2:S3:S4$ ratios for $h\nu=135$ eV are 2.4:1:3.1:1.6 and 4:1:3.9:2.2 at $\theta_e=0°$ and 60°, respectively, agreeing clearly with the atomic number ratio of $b1:b2:(a+c1):(c2+c3)$. Thus, the measured and calculated Si $2p$ results are in good agreement, supporting the structure of Fig. 1.

Next, the SCLS ranges measured for different Si reconstructions are worth comparing. In this study, the SCLS range for the Yb/Si(100)$(2\times6)$ is 0.66 eV. It is noticeably narrower than those of Yb/Si(100)$(2\times3)/(2\times4)$ [0.82 eV (Ref. 8)] and Eu/Si(100)$(2\times3)$ [1.05 eV (Ref. 9)], and it is smaller than that of the clean Si(100). Most likely, the difference is due to the lack of buckled Si dimers on the Yb/Si(100)$(2\times6)$ and the presence of such dimers on the Yb/Si(100)$(2\times3)/(2\times4)$, Eu/Si(100)$(2\times3)$, and clean Si(100) surfaces. In other words, the narrowed Si $2p$ emission from Yb/Si(100)$(2\times6)$ can be reasonably explained by the model of Fig. 1.

Now the question why the dimers are symmetrical in the $(2\times6)$ phase arises. In this study, in addition to the DFT calculations in Ref. 6, the $(2\times6)$ structure of Fig. 1 was retested by moving the dimer atoms into the "buckled" positions. After the full optimization of such a structure by VASP, the dimer buckling does not exceed 0.8 pm, meaning that the dimers are symmetrical on the Yb/Si(100)$(2\times6)$ with high precision. On the contrary, the fully optimized $(2\times3)$ and $(2\times4)$ structures of Yb/Si(100) contain one asymmetric dimer per surface unit.[6] In these structures, the uppermost Si layer is dimerized with three [four] dimers (one of which is buckled), and the Yb atoms donate four [six] electrons to the $(2\times3)$ $[(2\times4)]$ surface. On this basis, we suggest that the stabilization of the symmetrical dimer arrangement on Yb/Si(100) requires the charge transfer of two electrons from the metal to the substrate per dimer. In fact, in the $(2\times6)$ reconstruction there are five Si dimers and six Yb atoms that can donate 12 electrons to the surface per unit cell, and therefore, the total number of donated electrons is enough for the dimer symmetrization completely. Tentatively, the above two-electron transfer picture implies that two electrons donated from the metal saturate the half-filled dangling bonds of the dimer atoms, removing the charge rearrangement between the up and down atoms of a buckled dimer. The core-level binding-energy difference of the first- and topmost-layers dimer atoms in the $(2\times6)$ (i.e., the atoms $b1$ and $a$, respectively) is significant (0.3–0.4 eV). This infers that the atom $b1$ gains more electron charge than the atom $a$. The difference is thought to be due to that the distance between the atom $b1$ and the neighboring Yb atom is shorter than the distance between the atom $a$ and the neighboring Yb atom.

In conclusion, the Si $2p$ photoemission from the Yb/Si(100)$(2\times6)$ has been analyzed experimentally and theoretically. The initial state SCLS calculated for the structure in Fig. 1 agree well with the measured values, and the intensity ratios of Si $2p$ components are consistent with the number ratio of respective Si atoms, giving a strong support to the recently proposed atomic model. The relatively narrow Si $2p$ line shape for the Yb/Si(100)$(2\times6)$ is explained by the absence of buckled Si dimers in this reconstruction, in agreement with the valence-band measurements. It is suggested that the symmetrical dimer configuration is stabilized by the donation of two electrons from Yb per dimer.

We are grateful to H. Ollila and the MAX-lab staff for technical assistance. The financial supports by the Academy of Finland (Grants No. 122743 and No. 122355), Finnish Academy of Sciences and Letters, the Carl Tryggers Foundation (M.P.J.P.), the Emil Aaltonen Foundation (M.P.J.P.), and the Transnational Access to the Research Infrastructure Program (TARI) are kindly acknowledged. The calculations were performed using the facilities of the Finnish IT Center for Science (CSC).

*m.kuzmin@mail.ioffe.ru

[1] E. Landemark, C. J. Karlsson, Y.-C. Chao, and R. I. G. Uhrberg, Phys. Rev. Lett. **69**, 1588 (1992).
[2] E. Pehlke and M. Scheffler, Phys. Rev. Lett. **71**, 2338 (1993).
[3] R. I. G. Uhrberg, J. Phys.: Condens. Matter **13**, 11181 (2001).
[4] H. Koh, J. W. Kim, W. H. Choi, and H. W. Yeom, Phys. Rev. B **67**, 073306 (2003).
[5] P. E. J. Eriksson and R. I. G. Uhrberg, Phys. Rev. B **81**, 125443 (2010).
[6] M. P. J. Punkkinen, M. Kuzmin, P. Laukkanen, R. E. Perälä, M. Ahola-Tuomi, J. Lång, M. Ropo, M. Pessa, I. J. Väyrynen, K. Kokko, B. Johansson, and L. Vitos, Phys. Rev. B **80**, 235307 (2009).
[7] One ML is referred as to the atomic density on Si(100) $(6.78\times10^{14}$ atoms/cm$^2)$.
[8] M. Kuzmin, M. P. J. Punkkinen, P. Laukkanen, R. E. Perälä, M. Ahola-Tuomi, T. Balasubramanian, and I. J. Väyrynen, Phys. Rev. B **78**, 045318 (2008).
[9] M. Kuzmin, R. E. Perälä, P. Laukkanen, and I. J. Väyrynen, Phys. Rev. B **72**, 085343 (2005).
[10] M. V. Katkov and J. Nogami, Surf. Sci. **524**, 129 (2003).
[11] M. Kuzmin, R. E. Perälä, P. Laukkanen, R.-L. Vaara, M. A. Mittsev, and I. J. Väyrynen, Appl. Surf. Sci. **214**, 196 (2003).
[12] S. Zhu, J. Chen, M.-F. Li, S. J. Lee, J. Singh, C. X. Zhu, A. Du, C. H. Tung, A. Chin, and D. L. Kwong, IEEE Electron Device Lett. **25**, 565 (2004).
[13] L. S. O. Johansson, R. I. G. Uhrberg, P. Mårtensson, and G. V. Hansson, Phys. Rev. B **42**, 1305 (1990).
[14] G. Kresse and J. Hafner, Phys. Rev. B **47**, 558 (1993); **49**, 14251 (1994); G. Kresse and J. Furthmüller, Comput. Mater. Sci. **6**, 15 (1996); Phys. Rev. B **54**, 11169 (1996).
[15] P. E. Blöchl, Phys. Rev. B **50**, 17953 (1994); G. Kresse and D. Joubert, *ibid.* **59**, 1758 (1999).
[16] D. M. Ceperley and B. J. Alder, Phys. Rev. Lett. **45**, 566 (1980).
[17] J. P. Perdew and A. Zunger, Phys. Rev. B **23**, 5048 (1981).
[18] G. Kresse and J. Furthmüller, *Vienna Ab Initio Simulation Package, Users Guide* (The University of Vienna, Vienna, 2007).
[19] M. P. J. Punkkinen, K. Kokko, L. Vitos, P. Laukkanen, E. Airiskallio, M. Ropo, M. Ahola-Tuomi, M. Kuzmin, I. J. Väyrynen, and B. Johansson, Phys. Rev. B **77**, 245302 (2008).